Case Studies in Construction Materials 14 (2021) e00522

Contents lists available at ScienceDirect

Case Studies in Construction Materials

journal homepage: www.elsevier.com/locate/cscm

Case study

Case study on the optimal thickness of phase change material incorporated composite roof under hot climate conditions

Qudama Al-Yasiri[a,b,c,*], Márta Szabó[b]

[a] *Mechanical Engineering Doctoral School, Szent István University, Páter K. u. 1, Gödöllő, H-2100, Hungary*
[b] *Department of Building Services and Environmental Engineering, Faculty of Mechanical Engineering, Szent István University, Páter K. u. 1, Gödöllő, H-2100, Hungary*
[c] *Department of Mechanical Engineering, Faculty of Engineering, University of Misan Al Amarah City, Maysan Province, 62001, Iraq*

ARTICLE INFO

Article history:
Received 17 December 2020
Received in revised form 9 February 2021
Accepted 26 February 2021

Keywords:
PCM
Roof
Building energy
Decrement factor
Thermal performance
Time lag

ABSTRACT

The current study experimentally investigates the optimal thickness of a phase change material (PCM) layer incorporated composite roof under severe exterior temperatures. Three PCM thicknesses, namely 10, 15 and 20 mm, are embedded inside a popular roof combination for residential buildings in Iraq compared with the reference roof without PCM. The composite roof is composed of Isogam (4 mm) as a roofing material, concrete (50 mm) as a main roof layer, and gypsum board (8 mm) as a cladding layer, which is the worst thermal-performed roof combination in the country. Each PCM thickness case's thermal performance has been evaluated considering energetic indicators based on room temperature, interior surface temperature, and average outside surface temperature. These indicators are room maximum temperature reduction (RMTR), average temperature fluctuation reduction (ATFR), decrement factor (DF) and time lag (TL). The experimental results showed that the room temperature could be reduced by up to 9 °C compared with the reference roof. Moreover, the best thermal performance is reported for the composite roof based 20 mm thickness which resulted in a maximum of 13.9 % 10.74 °C, 44.7 % and 190 min of respectively RMTR, ATFR, DF and TL more than that of the reference case. The study concluded that the thicker PCM layer results in better thermal performance. However, increasing PCM thickness from 10 to 15 mm and then to 20 mm reduced RMTR by 2.3 % and 0.4 %, respectively. Therefore, the effect of PCM heat discharging medium and the economic concern should be considered when installing large PCM thickness/quantity into real scale buildings.

1. Introduction

In recent years, phase change materials (PCMs) incorporated building envelope have increasingly attracted attention as an energy-efficient solution in buildings. This booming technology has been proven remarkable enhancements in both energetic and thermal comfort features of buildings which make it an attractive building energy solution [1–3]. As a fast-growing technology, PCM incorporated buildings still under development considering different aspects such as investigating new PCM types, influential position within the envelope, optimal quantity, method of incorporation and best passive/active strategy to be utilised feasibly.

* Corresponding author at: Mechanical Engineering Doctoral School, Szent István University, Páter K. u. 1, Gödöllő, H-2100, Hungary.
E-mail address: qudamaalyasiri@uomisan.edu.iq (Q. Al-Yasiri).

https://doi.org/10.1016/j.cscm.2021.e00522

Studying the optimal PCM quantity/thickness to be incorporated with the building envelope is an intrinsic topic as it influences the thermal behaviour and mechanical properties of the building [4]. It is popularly known that increasing PCM quantity increases its heat storage capacity, which saves more energy. This concept is limited; for instance, a study reported that incorporating 5 mm of PCM layer into the roof was reduced the indoor peak temperature by 2 °C [5]. Whereas increasing the thickness from 5 mm to 10 mm and 15 mm was further reduced the indoor peak temperature by only 0.5 °C and 0.3 °C, respectively. From the other side, PCM quantity has a noticeable effect on the initial cost, determining the technology feasibility [6]. Likewise, this technology might not economically viable than the available insulation materials despite its thermal benefits [7]. For that, proper care has to be given to specify the optimal PCM quantity that gains the best thermal performance at a minimal cost.

Researchers have conducted several studies; the majority were numerical, to address this issue under different climatic conditions. For instance, Hagenau and Jradi [8] numerically studied 17 PCM types of melting temperature varied between 18 °C–26 °C and different thickness ranging from 5–100 mm under Danish weather conditions. Simulation results showed that the energy-saving, in terms of cooling and heating, was increased as the PCM thickness increase and the best effective thickness was 40 mm. At this thickness, the energy-saving reached 2.52 kW, whereas higher thicknesses lowered the cost-effectiveness. Hasan et al. [9] experimentally studied the effect of 1 and 2 cm PCM thicknesses on building thermal performance under Iraq's hot summer. Results were presented in terms of cooling load reduction and electricity saving for tested roof and walls. They concluded that PCM's best performance was at 1 cm thickness wherein the highest cooling load reduction of 20.9 % was achieved. Moreover, the maximum electricity saving of 1.35 USD/Day.m^3 was obtained at 1 cm PCM thickness incorporated all walls. Yu et al. [10] numerically studied the effect of shape stabilised PCM (melting temperature of 36 °C–38 °C) at different thicknesses, namely 20, 30, 40 and 50 mm integrated with building roof. They investigated the effective thickness in terms of inner surface temperature reduction and decrement factor. Results reported that the inner surface temperature was reduced when the thickness changed from 20 to 30 mm, and the decrement factor decreased as the PCM thickness increased. In conclusion, the PCM of 30 mm thickness decreased the inner surface temperature of the roof by 3.7 °C and reached a decrement factor of 85 %, compared with the roof without PCM. Li et al. [11] numerically studied the effect of increased thickness for two PCMs on a composite wall's thermal performance in Isfahan, Iran. They found out that increasing PCM thickness from 1 cm to 2 cm and then to 4 cm decreased the test wall's temperature and heat flux remarkably. They also concluded that increasing PCM thickness by two-fold was reducing the heat transfer to less than twofold. Tunçbilek et al. [12] studied the effect of PCM parameters, including layer thickness, on energy-saving under intermittent cooling in Marmara region, Turkey. Numerical results showed that the PCM of 23 mm thickness had the best thermal performance. Furthermore, a seasonal energy saving of 12.8 % was obtained from placing the PCM layer with this interior envelope's thickness. Yu et al. [13] performed a numerical analysis to study the effect of different PCMs having different thicknesses on roof's performance considering the decrement factor and peak inner roof surface temperature reduction under different regions of China. The outcomes showed that PCMs of 34 °C–38 °C melting temperature with 30 mm thickness were optimal to obtain a maximum decrement factor by 85 % and peak inner roof surface temperature reduction by 3.7 °C compared with a roof without PCM. Likewise, Wang et al. [14] found that the same thickness (i.e., 30 mm) can save energy by up to 27.78 % and 96.2 % respectively in summer and winter under Shanghai climatic weather conditions. Sovetova et al. [15] studied the energy-saving resulted from incorporating optimal PCM thickness into a residential building in Sharjah and Al-Ain, UAE. Numerical results showed that 20 mm PCM thickness reduced the maximum temperature by 1.09 °C. Moreover, the energy saved by 185.51 kW h and 211.24 kW h in Sharjah and Al-Ain, respectively, showing that the building based PCM can save up to 19 % less energy than the building without PCM. Arıcı et al. [16] numerically studied different PCM types considering different thicknesses under Turkish cities (namely Diyarbakır, Konya and Erzurum). The results indicated that PCMs of 6 °C–34 °C melting temperature were the best and the optimal thickness varied between 1–20 mm in which a time lag up to 13.3 h was obtained along with 18 % energy saving. In the same concept, Hu and Yu [17] studied the optimal thickness of the PCM integrated roof under five locations in China (Beijing, Heilongjiang, Nanjing, Guangzhou, and Kunming). Numerical results showed that the best PCM thickness varied between 5−25 mm and increasing PCM thickness by five times caused cooling load reduction by 2 %–7 %, and lowered the heating load consumption by 3 %–18 %, wherein the total energy saving reached 3 %–10 %.

Most of the literature studies were focused on PCM incorporated building walls, and minimal attention was given to the building roofs [18], as indicated in the studies mentioned above. Moreover, the building roof usually receives the majority of fallen solar radiation compared with walls, especially in flat roofs at hot climates. Therefore, the current research is conducted to provide more experimental investigations in this area of research.

In this paper, an experimental investigation on the optimal thickness of the PCM layer incorporated composite roof was performed under hot summer days in Iraq. Paraffin wax of 44 °C melting temperature served as PCM with three different quantities, namely 0.5, 0.75 and 1 kg, macroencapsulated using metal panels of 10, 15 and 20 mm thickness, respectively. Energetic indicators have been defined in terms of the test room temperature, interior roof surface temperature and average exterior roof temperature during peak hours to investigate the optimal thickness. Several conclusions were drawn from the results with some recommendations for further real-case study investigation.

2. Materials and methods

2.1. Experimental models

In the current work, 4 experimental test models (rooms) were installed on the rooftop of a residential building in Al Amarah city (Latitude: 31.84° & Longitude: 47.14°), Iraq, as shown in Fig. 1. The models are composed of a composite roof

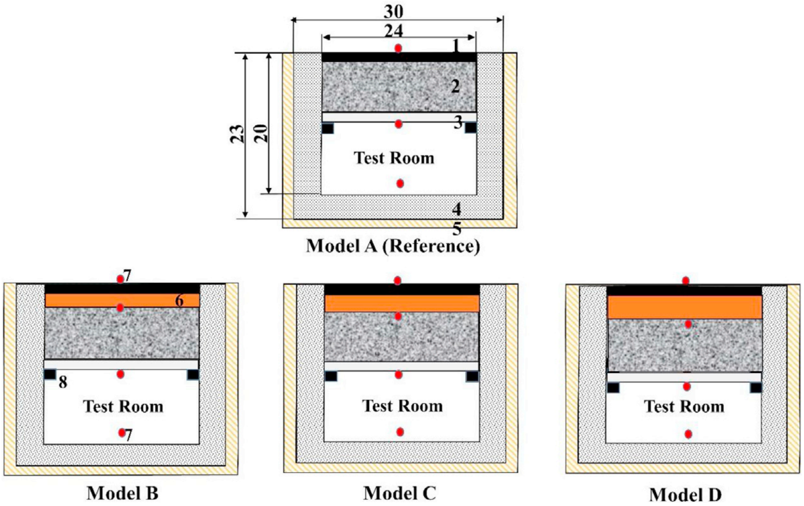

Fig. 1. Schematic for the experimental models.
(1- Finishing layer, 2- Main roof layer, 3- Cladding layer, 4- Box, 5- Insulation, 6- PCM layer, 7- Thermocouples, 8- Supporter).

situated inside a rectangular box. The box made from high-density cork characterised as the insulated floor and walls of the room. Moreover, high-density insulation blanket boxes were insulated to improve the insulation further and guarantee that the heat transfers only through the roof layers. The first model served as a reference room with a standard composite roof layers (Model A). The other three models were incorporated with an extra layer of macroencapsulated PCM panel with different thicknesses (Model B, Model C and Model D). The panels were placed beneath the roofing layer as it is the optimal position for the PCM within the building roof to gain the best thermal performance and energy-saving according to previous work investigated under the same hot climate conditions [19].

The composite roof consists of the following layers:

(i) *Isogam (finishing layer)*: Isogam is a local roofing layer used popularly in Iraq as an alternative to the traditional roofing layers such as the straw-clay and concrete tiles. It has recently been increasingly used due to its low cost, low weight compared with the other roofing options and excellent waterproofing. However, it has been reported that this roofing material has the worst thermal performance in terms of increased cooling loads [20]. The standard Isogam layer (0.4 mm thickness and 10 m long) composed of bitumen-rubber mastic and laminated from both sides with thin plastic layers. One of the layers coated with light-silver colour to reflect the fallen solar radiation and the other is melted by fire to stuck on the concrete roof during installation (Fig. 2a). The reflective layer is removable and highly influenced by changeable weather conditions, limiting its reflectivity after a short term of installation. Therefore, Isogam with removed reflective layer is used in the present work in order to test the PCM thermal behaviour at high exterior surface temperatures, which is the core of the present work.

(ii) *Concrete (main roof layer)*: Concrete layers of 50 mm thickness were fabricated according to mixing ratio 1:2:3 of the raw materials (cement: sand: gravel) that is popular used for residential building roofs in Iraq, providing compressive strength 25–30 Mpa [21,22]. The raw materials were mixed with water to fabricate the concrete mixture, which then poured into moulds and left dried naturally to form the concrete layers (Fig. 2b).

(iii) *Gypsum board (cladding layer)*: Pre-fabricated gypsum boards (8 mm thickness) were used in this work. Boards are made from gypsum (6 mm thickness) and laminated by thin carton sheets (1 mm) from both sides for strengthening. These

Fig. 2. Composite roof layers (a) photo for Isogam installation (b) concrete layers (c) gypsum boards.

Fig. 3. Preparation of PCM panels.

boards are popularly used for suspended ceilings and used in this work as they have adequate strength to carry the heavy-weight concrete layer along with high content of gypsum mortar that used for cladding in the Iraqi buildings (Fig. 2c).

2.2. PCM panels

Locally available paraffin wax served as a PCM in this work. This type of paraffin was extracted during the dewaxing process of Iraqi crude oil in the petroleum refineries [23]. Thus, it is widely available at low prices in the local market. Generally, paraffin has several desired properties such as safe operation, good thermal properties and high heat storage capacity, eco-friendly and compatible with diverse types of encapsulation materials [24]. The paraffin used in the current work has a melting temperature of 44 °C, thermal conductivity of 0.21 W/m K, latent heat of fusion of 190 kJ/kg, a density of 930 kg/m^3 in solid-state and 830 kg/m^3 in the liquid state, specific heat of 2.1 kJ/kg K for the solid and liquid states, respectively [9,25].

The PCM has been macroencapsulated using metal panels to be efficiently implemented and utilising its thermal storage potential. The panels were produced from a galvanised steel sheet (0.4 mm thickness) as it has high thermal conductivity, available in the local market and compatible with different PCMs, including paraffin [26]. The panels were fabricated with three thicknesses (10, 15 and 20 mm) and three quantities of paraffin, namely 0.5, 0.75 and 1 kg, were poured into them to be installed for Model B, Model C and Model D, respectively. The principal followed steps to prepare PCM panels are shown in Fig. 3.

It is worth to mention that the PCM panels were perfectly fit the poured PCM, and little space was left for two reasons. Firstly, to accommodate the expanded molten PCM during the charging phase and secondly to maintain leakage that might occur from inclined roof layers during roof installation. Furthermore, all roof layers were cleaned and smoothed to be contacted correctly. Furthermore, they were sealed, one by one, using high-quality insulation foam during installation to ensure no air infiltration between the interior and exterior environments during the experiment.

2.3. Measurement devices

The experiments lasted for three consecutive days (3-5/9/2020) starting from 6:00 on 3.9.2020 till 6:00 of 6.9.2020. A data logger based multi-channel Arduino (type Mega 2560) was used to record the temperatures through thermocouples. Fifteen thermocouples (T-type of 0.2 mm, ± 1 °C accuracy and ± 0.5 °C limits of error) were installed at different positions of the composite roof layers, namely on the outer surface of Isogam, beneath the PCM layer, beneath the gypsum layer and inside the test room, as indicated in Fig. 1. The data logger was programmed to record the temperatures every 10 min to overcome all temperature fluctuation during the experiment days. Then, the recorded temperatures are instantly saved into 4 GB storage memory. During day-hours, the solar radiation was collected manually every 30 min using a solar power meter (Model SM206) with 10 W/m^2 accuracy and 0.1 W/m^2 resolution. Measurement devices and their installation on the experimental models are shown in Fig. 4.

2.4. Assessment of PCM thermal performance

Four energetic indicators have been introduced to evaluate each PCM model's thermal performance compared with the reference model and specify the optimal thickness, accordingly. These indicators are room maximum temperature reduction,

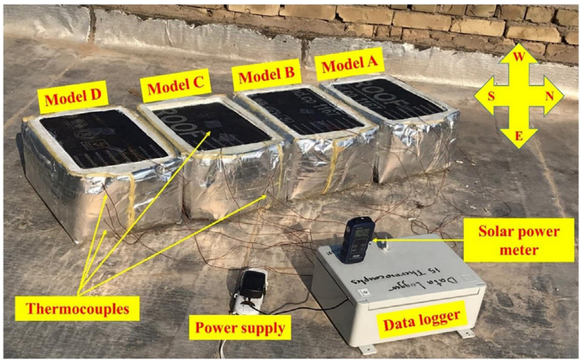

Fig. 4. Experimental set-up.

average temperature fluctuation reduction, decrement factor and time lag. The indicators were considered the test room temperature (T_r), interior surface temperature (T_i) and the average exterior surface temperature of the roof (T_o) to evaluate the energy improvement gained from incorporating the different thickness PCM layers into the composite roof.

3. Results and discussion

Fig. 5 shows the experimental models' temperature profile (Model A, Model B, Model C and Model D) as a function of time during days of the experiment. In the early hours of each day, T_r is higher than T_o due to low solar radiation. Later, the temperatures increased with the solar radiation (SR) increase and reached the maximum around 13:00 in each day-cycle. The maximum T_o achieved was 72.7 °C, 76.9 °C and 67.9 °C respectively in the first, second and third day of experiment encountered with the highest SR of 1149, 1210 and 1139 W/m^2, respectively. It is worth mentioning that the experimental

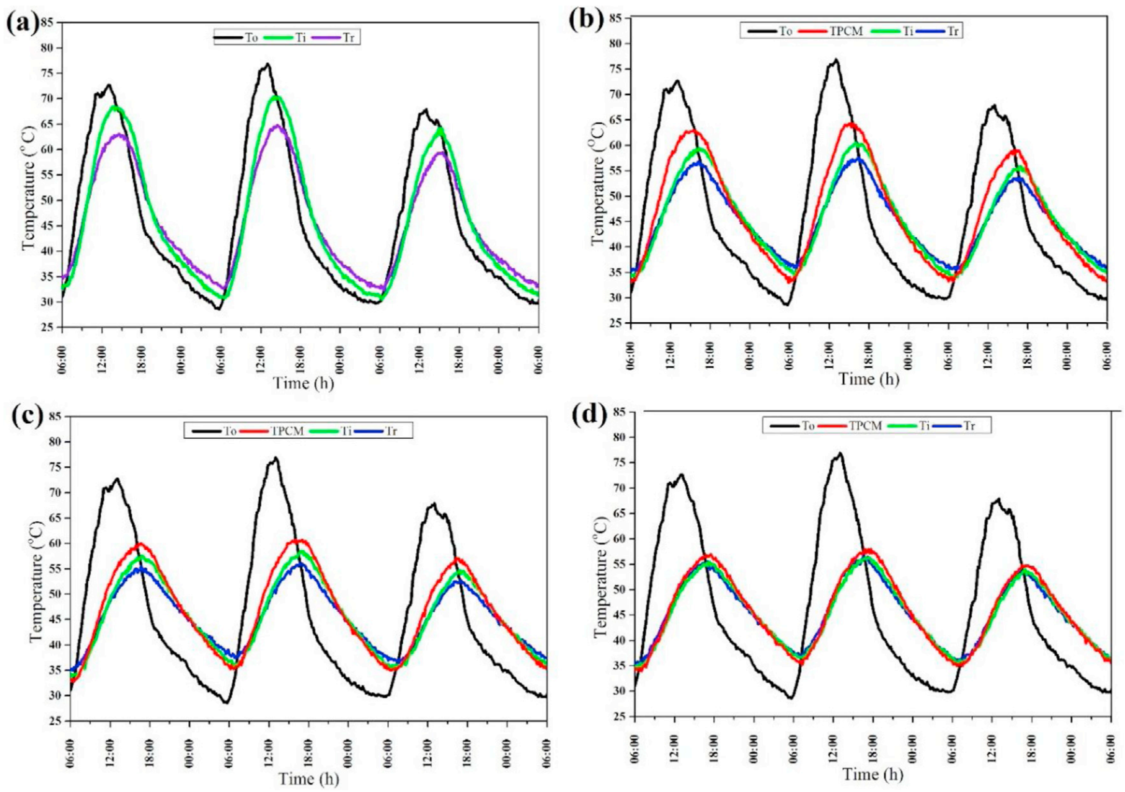

Fig. 5. Temperature profile of tested models (a) Model A (b) Model B (c) Model C (d) Model D.

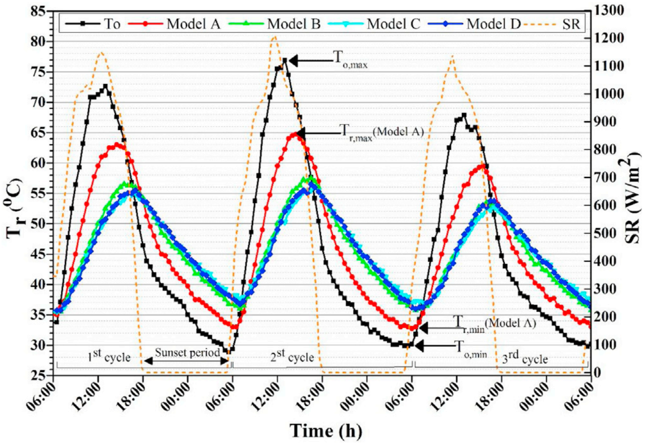

Fig. 6. T_r profile of experimental models.

work has experienced some hours of partially-clouded weather in the midday, especially on the first and third days of the experiment.

In general, T_i and T_r in PCM models were lower than those of the reference model due to PCM heat storage capacity. In this regard, T_i and T_r were decreased as the thickness of the PCM layer increased, which shows the PCM ability to shave the temperature fluctuations during peak hours.

During the night period, T_o values were falling quickly as the SR decreased until it disappeared around 18:00 each day. T_o was fallen sharply followed by T_{PCM} for PCM models with a slight reduction in T_i and T_r temperature profiles. The lower T_o - between 28.6 °C–29.75 °C - has been recorded during the late night of the experiment, which was suitable for discharging the heat from PCM models passively and prepare them for the next day cycle.

As mentioned in Section 2.4, there have been several indicators applied to analyse the thermal performance of each PCM model compared with the reference model, as follows:

3.1. Room maximum temperature reduction (RMTR)

It has been proven that PCM can reduce the indoor temperature thanks to its thermal storage potential. As shown in Fig. 6, the PCM of different thicknesses remarkably reduced the room temperature during peak hours. The maximum T_r was achieved in the second cycle as 64.75 °C, 57.5 °C, 56 °C, 55.75 °C in Model A, Model B, Model C and Model D, respectively against a maximum T_o of 76.9 °C. This signifies a reduction of 7.25 °C, 8.75 °C and 9 °C for Model B, Model C and Model D compared with the reference case (i.e., Model A).

RMTR indicates how considerable is the reduction of the temperature inside the test room for each PCM model during peak hours. This indicator clearly shows the utilisation of each PCM thickness's storage capacity and whether or not the PCM

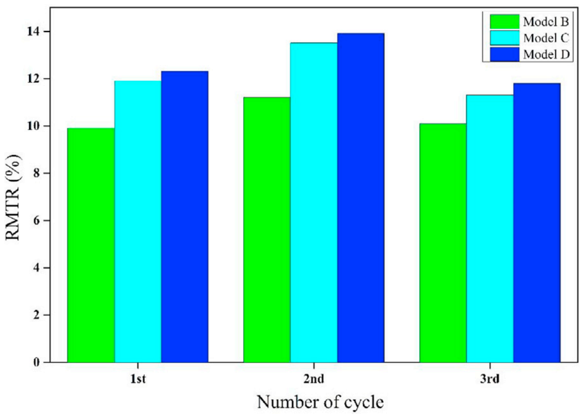

Fig. 7. RMTR for PCM models.

fully melted. To do so, RMTR is calculated by considering the maximum room temperature of PCM model compared with the reference room by using Eq. (1), as follows:

$$RMTR = \frac{T_{r,max.,\ ref.} - T_{r,\ max.\ ,PCM}}{T_{r,max.\ ,ref.}} \times 100\% \tag{1}$$

where $T_{r,max.,ref.}$ and $T_{r,max.,PCM}$ are the maximum temperature of T_r for Model A and PCM models, respectively. The calculated RMTR of PCM models is shown in Fig. 7.

Model D has the best RMTR compared with the other PCM models. The better performance obtained at the second cycle indicates a better utilisation of PCM thermal storage at higher temperatures resulting from using PCM of high melting temperature. At this cycle, a maximum RMTR of 11.2 %, 13.5, and 13.9 % for Model B, Model C and Model D were calculated at the highest T_o. It means that increasing PCM thickness from 10 to 15 mm was reduced T_r by 2.3 % whereas, increasing the thickness from 15 to 20 mm was reduced T_r by 0.4 % only.

3.2. Average temperature fluctuation reduction (ATFR)

ATFR is the average decrement of test room temperature fluctuations during the day and night period. As we deal with non-conditioned rooms, ATFR can be calculated by combining the average decrease in room temperature in the day hours (X) (i.e., from 6:00 to 18:00) with the average increase in room temperature in the night period (Y) (i.e., from 18:00 to the end of day cycle at 6:00), according to Eqs. (2)–(4), as follows [27]:

$$\mathrm{ATFR} = X + Y \tag{2}$$

$$X = T_{r,av.,ref.} - T_{r,av.,\ PCM} \tag{3}$$

$$Y = T_{r,av.,\ PCM} - T_{r,av.,\ ref.} \tag{4}$$

where $T_{r\ av.,ref.}$ is the average temperature of the reference room (Model A), and $T_{r\ av.,PCM}$ is the average temperature of PCM rooms (i.e., Model B, Model C and Model D) (°C). The calculated results of ATFR are shown in Fig. 8.

The results showed that ATFR was high for Model C compared with Model B and Model D where the maximum value obtained in the first day-cycle was 8.75 °C, 10.98 °C and 10.74 °C for Model B, Model C and Model D, respectively. The reason attributes to the effect of passive incorporation on the solidification phase during night hours in which the stored heat in Model D was not released totally. The calculation of ATFR values in all cycles showed that X value was higher for Model D than Model B and Model C. In reverse, the value of Y was much high for Model C than Model B and Model D. Therefore, the summation of X and Y resulted in higher ATFR for Model C than Model B and Model D. This indicator informs us that the thicker PCM (i.e. 20 mm) can save more heat during day hours and reduce the room temperature. However, at the same time, it has lower thermal performance during the night time and could not release all stored heat, passively. The main reason behind that is the low thermal conductivity of PCMs in nature, paraffin in particular, which slow down the time to reach full melting and solidification. Several techniques were reported in the literature to enhance the low thermal conductivity of PCMs using different enhancers such as the use of fins, metallic foams and presence of nanoparticles [28,29].

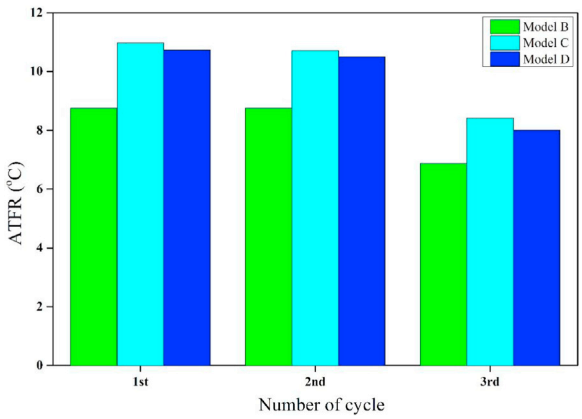

Fig. 8. ATFR of PCM models.

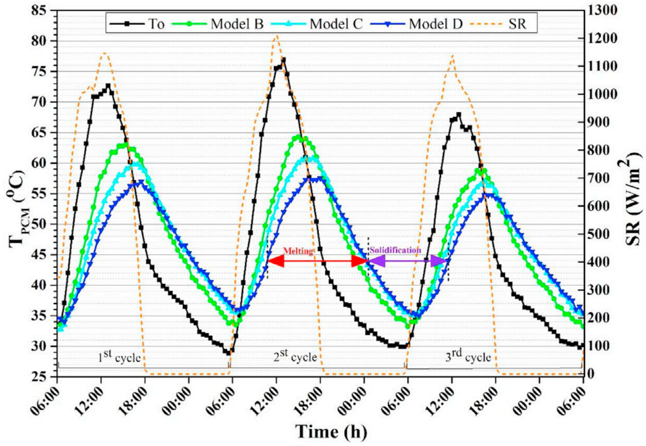

Fig. 9. T_{PCM} profile of experimental models.

ATFR results indicated a high thermal performance of PCM in the present work in which the values were in the range 6 °C < ATFR < 11 °C, which is much higher than the results reported in the literature. For instance, a study reported that the value of ATFR ranged between 3 °C–4 °C under the Australian climate conditions [30].

As the value of ATFR influenced by the temperatures during the daytime and nighttime, it is worth to analyse the thermal performance of PCM in each PCM model. As shown in Fig. 9, it can be realised that the T_{PCM} in all PCM models was increased as the SR increase and decreased at lower SR and night period. Model B showed a faster increase in T_{PCM} which was close to T_o followed by the Model C and then, Model D. This is logical meaning that the PCM melted earlier in Model B because of its little quantity, and the heat later passed towards the test room. Consequently, the heat took more time to pass through Model C and Model D that had more PCM quantity to be melted. Considering the melting temperature of used PCM (i.e., 44 °C), we can say that the PCM melted earlier in Model B than Model C and Model D around 9:00, 10:00 and 11:00, respectively, in the first-day cycle.

On the other hand, during the solidification period, the TPCM of Model B was the closest to To meaning that the thickness of PCM was solidified faster in Model B than the other models. Likewise, the solidification in Model C was a bit faster than Model D due to its lower PCM quantity. Accordingly, the lower the PCM quantity, the faster to be solidified.

3.3. Decrement factor (DF)

DF stands for the decrease of roof peak temperature in each model, considering the interior and exterior surface temperatures. Therefore, it is calculated using Eq. (5), as follows [31]:

$$DF = \frac{T_{i,max} - T_{i,\min}}{T_{o,max} - T_{o,\min}} \tag{5}$$

where $T_{i,max}$, $T_{i,min}$, $T_{o,max}$ and $T_{o,min}$ are the maximum and minimum temperatures of the roof's interior and exterior surfaces (°C), respectively. In this regard, lower DF value means lower cyclic fluctuations in the interior surface temperature during

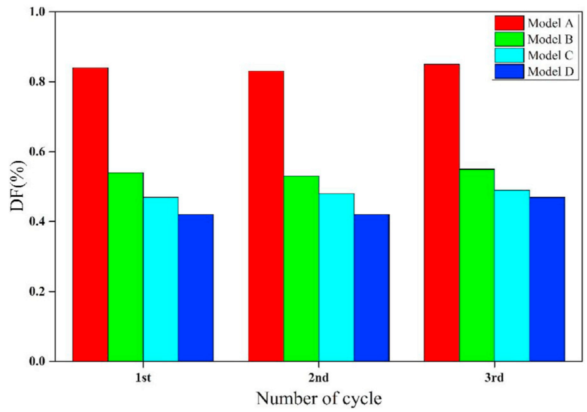

Fig. 10. DF of experimental models.

day-cycle as an advantage of PCM thermal storage capacity. Fig. 10 shows the calculated values of DF for experimental models.

As shown in the figure and compared with Model A, Model D has the best DF in all cycles followed by Model C and then Model B. The maximum DF was obtained in the third day-cycle, which was 0.85, 0.55, 0.49 and 0.47 for Model A, Model B, Model C and Model D, respectively. That means reducing the cyclic interior surface temperature by 35.3 %, 42.4 % and 44.7 % for Model B, Model C and Model D compared with Model A. This reduction positively influences thermal comfort in real case studies as it affects the mean radiant temperature and operative temperature [32].

3.4. Time lag (TL)

TL is simply defined as the period to reach maximum T_i considering the maximum T_o. This indicator shows the shifting of peak load to off-load hours. Therefore, it can be calculated as the difference between the time at maximum interior surface temperature ($T_{i,max}$) and the time at maximum outer surface temperature ($T_{o,max}$), according to Eq. (6) [33], as follows:

$$TL = \tau_{\,T_{i,max}} - \tau_{T_{o,max}} \tag{6}$$

where $\tau_{Ti,max}$ and $\tau_{To,max}$ are the time at the maximum interior and exterior surface temperatures of the roof (min), respectively. The TL obtained from each model in all cycles is shown in Fig. 11.

As indicated in the figure, peak hours were shifted in all PCM models to the late time compared with the reference model. Results showed that the TL ranged between 80–130 min for Model A, 180–220 min for Model B, 230–240 min for Model C and from 240 to 270 for Model D. The highest TL for Model D was obtained in the second day-cycle at the highest T_o in the experiment. At this cycle, the time in Model B, Model C and Model D was extended by 100 min, 150 min and 190 min respectively compared with Model A.

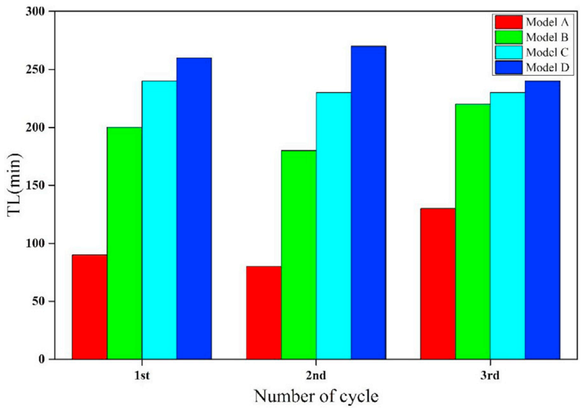

Fig. 11. TL of the experimental models.

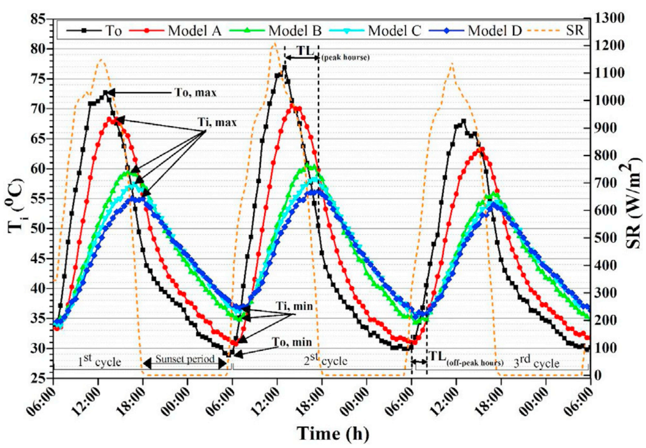

Fig. 12. T_i profile for experimental models.

It is well known that TL can be calculated for the crests during peak and off-hours, as shown in Fig. 12. The TL during peak hours is more important because they show the shifting of high temperatures as an advantage of incorporating the PCM layer. Moreover, after the SR drops, a higher reduction in the interior surface temperatures also can be recognised during daytime compared with the nighttime.

TL together with the DF is essential to study PCM's influence on the thermal performance of building envelope because they show how the building envelope restricted the high outside temperatures that are not felt inside buildings [34].

4. Conclusions

The main objective of the current study is to experimentally identify the optimal thickness of the PCM layer incorporated composite roof, passively. The study was conducted under sever hot climate conditions of Iraq for a popular roof combination (i.e., Isogam-concrete-gypsum) which is the worst option in the residential building installations in terms of cooling loads. Four test models were used for this purpose in which the first model composed of the regular roof combination, and the other integrated with PCM panel of 10, 15 and 20 mm, respectively.

The study reported that the thicker PCM thickness results in better thermal performance, and the room temperature can be reduced as high as 9 °C using 20 mm PCM thickness. Furthermore, the best thermal performance was reported for this thickness in terms of room maximum temperature reduction, decrement factor and time lag as 13.9 % 10.74 °C, 44.7 % and 190 min, respectively. It worth to mention that these results are too close to those obtained at 15 mm thickness. For instance, increasing PCM thickness from 10 to 15 mm reduced T_r by 2.3 % whereas, increasing the thickness from 15 to 20 mm was reduced T_r by only 0.4 %.

Thicker PCM layer (i.e., 20 mm) showed poor thermal performance considering the average temperature fluctuation reduction. For instance, ATFR values of Model C were 10.98 °C, 10.72 °C and 8.42 °C compared with 10.74 °C, 10.5 °C and 8.01 °C for Model D, respectively. This shows a worse thermal performance of Model D because the stored heat in the day did not release fast during the night period and affected the room temperature throughout the day. Therefore, the optimal thickness of PCM integrated real building scale in a passive manner should be studied considering the heat discharging medium as well as the economic concerns.

Declaration of Competing Interest

The authors declare that they have no known competing financial interests or personal relationships that could have appeared to influence the work reported in this paper.

Acknowledgements

This work was supported by the Stipendium Hungaricum Programme and the Mechanical Engineering Doctoral School, Szent István University, Gödöllő, Hungary.

References

[1] P.K. Singh Rathore, S.K. Shukla, N.K. Gupta, Potential of microencapsulated PCM for energy savings in buildings: A critical review, Sustain. Cities Soc. 53 (2020)101884, doi:http://dx.doi.org/10.1016/j.scs.2019.101884.

[2] Q. Al-Yasiri, M. Szabó, Incorporation of phase change materials into building envelope for thermal comfort and energy saving: A comprehensive analysis, J. Build. Eng. 36 (2021)102122, doi:http://dx.doi.org/10.1016/j.jobe.2020.102122.

[3] E. Tunçbilek, M. Arıcı, S. Bouadila, S. Wonorahardjo, Seasonal and annual performance analysis of PCM-integrated building brick under the climatic conditions of Marmara region, J. Therm. Anal. Calorim. 141 (2020) 613–624, doi:http://dx.doi.org/10.1007/s10973-020-09320-8.

[4] U. Berardi, A.A. Gallardo, Properties of concretes enhanced with phase change materials for building applications, Energy Build. 199 (2019) 402–414, doi:http://dx.doi.org/10.1016/j.enbuild.2019.07.014.

[5] Y. Zhang, J. Huang, X. Fang, Z. Ling, Z. Zhang, Optimal roof structure with multilayer cooling function materials for building energy saving, Int. J. Energy Res. 44 (2020) 1594–1606, doi:http://dx.doi.org/10.1002/er.4969.

[6] E. Kyriaki, C. Konstantinidou, E. Giama, A.M. Papadopoulos, Life cycle analysis (LCA) and life cycle cost analysis (LCCA) of phase change materials (PCM) for thermal applications: A review, Int. J. Energy Res. 42 (2018) 3068–3077, doi:http://dx.doi.org/10.1002/er.3945.

[7] A. Baniassadi, B. Sajadi, M. Amidpour, N. Noori, Economic optimisation of PCM and insulation layer thickness in residential buildings, Sustain. Energy Technol. Assess. 14 (2016) 92–99, doi:http://dx.doi.org/10.1016/j.seta.2016.01.008.

[8] M. Hagenau, M. Jradi, Dynamic modeling and performance evaluation of building envelope enhanced with phase change material under Danish conditions, J. Energy Storage 30 (2020)101536, doi:http://dx.doi.org/10.1016/j.est.2020.101536.

[9] M.I. Hasan, H.O. Basher, A.O. Shdhan, Experimental investigation of phase change materials for insulation of residential buildings, Sustain. Cities Soc. 36 (2018) 42–58, doi:http://dx.doi.org/10.1016/j.scs.2017.10.009.

[10] J. Yu, Q. Yang, H. Ye, Y. Luo, J. Huang, X. Xu, W. Gang, J. Wang, Thermal performance evaluation and optimal design of building roof with outer-layer shape-stabilised PCM, Renew. Energy 145 (2020), doi:http://dx.doi.org/10.1016/j.renene.2019.08.026.

[11] Z.X. Li, A.A.A.A. Al-Rashed, M. Rostamzadeh, R. Kalbasi, A. Shahsavar, M. Afrand, Heat transfer reduction in buildings by embedding phase change material in multi-layer walls: Effects of repositioning, thermophysical properties and thickness of PCM, Energy Convers. Manage. 195 (2019) 43–56, doi:http://dx.doi.org/10.1016/j.enconman.2019.04.075.

[12] E. Tunçbilek, M. Arıcı, M. Krajčík, S. Nižetić, H. Karabay, Thermal performance based optimisation of an office wall containing PCM under intermittent cooling operation, Appl. Therm. Eng. 179 (2020)115750, doi:http://dx.doi.org/10.1016/j.applthermaleng.2020.115750.

[13] J. Yu, Q. Yang, H. Ye, Y. Luo, J. Huang, X. Xu, W. Gang, J. Wang, Thermal performance evaluation and optimal design of building roof with outer-layer shape-stabilised PCM, Renew. Energy 14 (2020) 2538–2549, doi:http://dx.doi.org/10.1016/j.renene.2019.08.026.

[14] H. Wang, W. Lu, Z. Wu, G. Zhang, Parametric analysis of applying PCM wallboards for energy saving in high-rise lightweight buildings in Shanghai, Renew. Energy 145 (2020) 52–64, doi:http://dx.doi.org/10.1016/j.renene.2019.05.124.
[15] M. Sovetova, S.A. Memon, J. Kim, Energy savings of pcm-incorporated building in hot dry climate, Key Eng. Mater. 821 (2019) 518–524, doi:http://dx.doi.org/10.4028/www.scientific.net/KEM.821.518 KEM.
[16] M. Arıcı, F. Bilgin, S. Nižetić, H. Karabay, PCM integrated to external building walls: An optimisation study on maximum activation of latent heat, Appl. Therm. Eng. 165 (2020)114560, doi:http://dx.doi.org/10.1016/j.applthermaleng.2019.114560.
[17] J. Hu, X. (Bill) Yu, Adaptive building roof by coupling thermochromic material and phase change material: Energy performance under different climate conditions, Constr. Build. Mater. 262 (2020), doi:http://dx.doi.org/10.1016/j.conbuildmat.2020.120481.
[18] L.F. Cabeza, L. Navarro, A.L. Pisello, L. Olivieri, C. Bartolomé, J. Sánchez, S. Álvarez, J.A. Tenorio, Behaviour of a concrete wall containing micro-encapsulated PCM after a decade of its construction, Sol. Energy 200 (2020) 108–113, doi:http://dx.doi.org/10.1016/j.solener.2019.12.003.
[19] Q. Al-Yasiri, M. Szabó, Experimental evaluation of the optimal position of a macroencapsulated phase change material incorporated composite roof under hot climate conditions, Sustain. Energy Technol. Assess. 45 (2021) 101121, doi:http://dx.doi.org/10.1016/j.seta.2021.101121.
[20] Q. Al-Yasiri, M.A. Al- Furaiji, A.K. Alshara, Comparative study of building envelope cooling loads in Al-Amarah city, Iraq, J. Eng. Technol. Sci. 51 (2019) 632–648, doi:http://dx.doi.org/10.5614/j.eng.technol.sci.2019.51.5.3.
[21] Thermal Insulation Blog (Iraqi Construction Blog)- The Ministry of Construction, Housing Municipalities and Public Work, (2013) https://amanatbaghdad.gov.iq/amanarules/pict/مدونات/blog20-مدونة العزل الحراري.pdf.
[22] S.F. Resan, S.M. Chassib, S.K. Zemam, M.J. Madhi, New approach of concrete tensile strength test, Case Stud. Constr. Mater. 12 (2020) 1–13, doi:http://dx.doi.org/10.1016/j.cscm.2020.e00347.
[23] H.J. Akeiber, M.A. Wahid, H.M. Hussen, A.T. Mohammad, A newly composed paraffin encapsulated prototype roof structure for efficient thermal management in hot climate, Energy 104 (2016) 99–106.
[24] A. Reza Vakhshouri, Paraffin as phase change material, in: F.S. Soliman (Ed.), Paraffin - an Overv., IntechOpen, 2019, doi:http://dx.doi.org/10.5772/intechopen.90487.
[25] M.T. Chaichan, A.H. Al-Hamdani, A.M. Kasem, Enhancing a Trombe wall charging and discharg- ing processes by adding nano-Al2O3 to phase change materials, Int. J. Sci. Eng. Res. 7 (2016) 736–741. http://www.ijser.org.
[26] G.H. Feng, D. Liang, K.L. Huang, Y. Wang, Thermal performance difference of phase change energy storage units based on tubular macro-encapsulation, Sustain. Cities Soc. 50 (2019)101662, doi:http://dx.doi.org/10.1016/j.scs.2019.101662.
[27] S. Kenzhekhanov, S.A. Memon, I. Adilkhanova, Quantitative evaluation of thermal performance and energy saving potential of the building integrated with PCM in a subarctic climate, Energy 192 (2020)116607, doi:http://dx.doi.org/10.1016/j.energy.2019.116607.
[28] Z.A. Qureshi, H.M. Ali, S. Khushnood, Recent advances on thermal conductivity enhancement of phase change materials for energy storage system: A review, Int. J. Heat Mass Transf. 127 (2018) 838–856, doi:http://dx.doi.org/10.1016/j.ijheatmasstransfer.2018.08.049.
[29] D. Li, Y. Wu, C. Liu, G. Zhang, M. Arıcı, Energy investigation of glazed windows containing Nano-PCM in different seasons, Energy Convers. Manage. 172 (2018) 119–128, doi:http://dx.doi.org/10.1016/j.enconman.2018.07.015.
[30] M. Alam, H. Jamil, J. Sanjayan, J. Wilson, Energy saving potential of phase change materials in major Australian cities, Energy Build. 78 (2014) 192–201, doi:http://dx.doi.org/10.1016/j.enbuild.2014.04.027.
[31] C. Sun, S. Shu, G. Ding, X. Zhang, X. Hu, Investigation of time lags and decrement factors for different building outside temperatures, Energy Build. 61 (2013) 1–7, doi:http://dx.doi.org/10.1016/j.enbuild.2013.02.003.
[32] ANSI/ASHRAE Standard 55-2010, Thermal environmental conditions for human occupancy, Encycl. Finance (2010), doi:http://dx.doi.org/10.1007/0-387-26336-5_1680.
[33] A. Thongtha, A. Khongthon, T. Boonsri, C. Hoy-Yen, Thermal effectiveness enhancement of autoclaved aerated concrete wall with PCM-contained conical holes to reduce the cooling load, Materials (Basel) 12 (2019) 2170, doi:http://dx.doi.org/10.3390/ma12132170.
[34] P.M. Toure, Y. Dieye, P.M. Gueye, V. Sambou, S. Bodian, S. Tiguampo, Experimental determination of time lag and decrement factor, Case Stud. Constr. Mater. 11 (2019)e00298, doi:http://dx.doi.org/10.1016/j.cscm.2019.e00298.